Optics Communications 324 (2014) 30–33

Contents lists available at ScienceDirect

Optics Communications

journal homepage: www.elsevier.com/locate/optcom

Dark-ground imaging of high optical thickness atom clouds

Aaron Reinhard [a,*], Jean-Félix Riou [b], Laura A. Zundel [b], David S. Weiss [b]

[a] Department of Physics, Otterbein University, 1 South Grove St., Westerville, OH 43081, USA
[b] Physics Department, The Pennsylvania State University, 104 Davey Lab, University Park, PA 16802, USA

ARTICLE INFO

Article history:
Received 21 December 2013
Received in revised form
26 February 2014
Accepted 28 February 2014
Available online 14 March 2014

Keywords:
Imaging ultracold atoms
Bose-Einstein condensation
Dark-ground imaging

ABSTRACT

We use resonant dark-ground imaging to obtain in situ images of Bose Einstein condensates with optical thicknesses up to 350. Our technique is easy to implement and the detected signal is large. We discuss the regimes of applicability of this method as well as its limitations.

Imaging is the dominant way to gain information about a sample of ultracold atoms. Images of atom clouds may be taken either in situ or after ballistic expansion. They can be used to access a wide variety of information about an evolving cloud of ultracold atoms, including position and momentum distributions [1–4], coherence properties [5,6], and quasimomentum distributions [7]. Techniques for imaging ultracold atom clouds can be placed into three broad categories: fluorescent, absorptive, and dispersive. For imaging low density clouds, on-resonance fluorescence or absorption with low probe intensities is often employed. These techniques are not easy to use for dense atomic clouds, since probe beam absorption makes atoms see a nonuniform probe intensity along the direction of the beam. Low intensity absorption imaging of small clouds further suffers from distortion of the image due to "lensing" caused by the atoms' index of refraction and the cloud's small radius of curvature.

Atomic clouds with optical thickness much larger than one, such as in situ Bose-Einstein condensates (BECs) or degenerate Fermi gases, are often imaged using dispersive techniques [8–10]. These techniques rely on the interference of phase shifted probe light with unshifted light. Because the probe is highly detuned from resonance, these techniques do not suffer significantly from image distortion due to lensing or from probe saturation. Dispersive imaging is often the most attractive technique for imaging dense clouds, although it does require a highly detuned (hundreds of atomic linewidths) probe beam and involves nontrivial image processing. Resonant fluorescence from a high intensity probe beam can also be used to image dense clouds [11]. While fluorescent imaging is robust and requires no signal processing, it suffers from a smaller signal than other imaging techniques. This is because in fluorescent imaging, one collects a fraction of all scattered light, while in other techniques one collects the entire signal imprinted on the probe beam.

Both absorptive and dispersive imaging techniques can be implemented in a "dark-ground" geometry in which spatial filtering is employed to remove the unscattered probe beam in the Fourier plane of a one-to-one imaging system [8,12,13]. Dark-ground imaging techniques have advantages for the extreme cases of low atom number or high optical depth clouds. The low atom number case has been treated previously [13]. It was shown that photon shot noise of the probe beam limits the signal-to-noise in absorption images of small atom number clouds. Because resonant dark-ground imaging eliminates the probe beam from the image, it significantly improves the images' signal-to-noise [13]. Here, we extend resonant dark-ground imaging to the regime of high optical depth samples, observing atomic clouds with optical thicknesses (OT) in the hundreds. Our technique was used previously to study the self-trapping dynamics of quasi-1D gases in a 2D optical lattice [14]. The technique is simple to implement, has high signal-to-noise, and requires minimal image processing compared to dispersive imaging. However, it requires a very high intensity probe, it involves a reduction of the resolution by a factor $\sqrt{2}$ and there is a small amount of density-dependent distortion at very high densities (although the distortion is smaller than for low-intensity absorption imaging).

In our experiment, a resonant probe beam of intensity I_o and $1/e^2$ waist 1.3 mm impinges on a ^{87}Rb BEC and continues through the imaging system shown schematically in Fig. 1. When $I_o \gg OT \times I_s$, where I_s is the saturation intensity, all the atoms spontaneously emit at the maximum rate, and the probe intensity is decreased by an amount proportional to the integrated atom

* Corresponding author.
E-mail address: areinhard@otterbein.edu (A. Reinhard).

http://dx.doi.org/10.1016/j.optcom.2014.02.070
0030-4018/

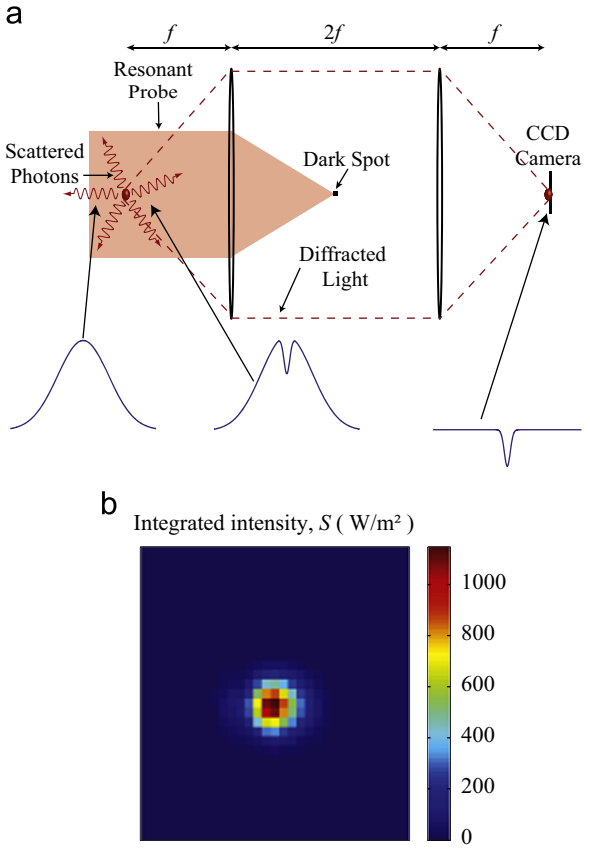

Fig. 1. (a) Schematic illustration of the imaging system used for high intensity absorption imaging, where f is the focal length of the lenses. Photons are resonantly scattered out of the probe beam by the atom cloud. Diffracted probe light within the cone illustrated by dotted lines is imaged on the camera, while the incident beam is blocked by a dark spot. At the bottom of the figure, we show the transverse electric field profile of the probe beam at various points in the imaging system. The size of the cloud relative to the beam waist has been exaggerated for clarity. (b) A sample image of the Bose Einstein condensate used for Fig. 2, taken with a probe intensity of $I/I_s = 632$. The pixel size is 3.33 μm.

density along a line. Because the light intensity is far above saturation, the ground and excited state populations are nearly equal, which suppresses non-linear effects [15]. We block the undiffracted part of the probe using a 400 μm diameter "dark spot" in the focal plane, and collect the diffracted light with a one-to-one imaging system (see Fig. 1a). Light energy proportional to the integrated atom density is spontaneously scattered from the probe, which causes a dip in the electric field amplitude of the probe beam. When the undiffracted part of the probe beam is blocked, the image formed by the remaining light has the shape of the dip. We note that our technique is different from a previously reported high intensity absorption imaging technique in which the "standard" absorption imaging geometry was used with probe beams about 40 times less intense than the ones used here [16]. Since the probe beam in that case had to be filtered before the camera to prevent saturation, the per atom signal was reduced as the OT increased. It is unchanged here.

We now derive the light intensity at the output of our imaging system as a function of the 2D integrated atomic density. We denote the electric field of the incident probe beam as $\vec{E}_o$, the decrease in electric field due to spontaneous emission as $\vec{E}_{dip}$, and the field transmitted through the atoms as $\vec{E}_{prop}$. By the superposition principle,

$$\vec{E}_{prop} = \vec{E}_o - \vec{E}_{dip}. \tag{1}$$

By conservation of energy,

$$I_{prop} = I_o - I_{scat}. \tag{2}$$

where I_{scat} is the part of the incident intensity that is spontaneously scattered out of the probe beam, and I_{prop} is the intensity of the probe beam immediately after passing through the atoms. Note that only in the limit of a completely black absorber, where $I_{prop} = 0$, is I_{scat} is proportional to $|\vec{E}_{dip}|^2$. It is easy to show that

$$I_{scat} = I_s \sigma_o n_{2D}(x,y), \tag{3}$$

where I_s is the saturation intensity, σ_o is the resonant scattering cross section, and $n_{2D}(x,y)$ is the 3D density distribution integrated along the line of sight.

Using $I = (c\epsilon_o/2)|\vec{E}|^2$ in free space, we can combine Eqs. (1) and (2) to obtain

$$E_{dip} = E_o - \sqrt{E_o^2 - \frac{2}{c\epsilon_o} I_{scat}}. \tag{4}$$

Since $I_o \gg I_s$, $E_o^2 = (2/c\epsilon_o) I_o \gg (2/c\epsilon_o) I_{scat}$ and we may expand the square root to first order to obtain

$$E_{dip} \approx \frac{1}{c\epsilon_o} \frac{I_{scat}}{E_o}. \tag{5}$$

Because of the dark spot, only $-\vec{E}_{dip}$ propagates through the entire imaging system. The intensity detected on the CCD is

$$I_{sig} \approx \frac{1}{4} \frac{I_{scat}^2}{I_o}. \tag{6}$$

As shown in Fig. 1b, we detect a bright image on the CCD due to the dip in the probe electric field caused by light being scattered out of the probe beam. Our technique relies on the fact that a dip in the electric field of the beam gives the same diffraction pattern as an electric field which has the shape of the dip. This is reminiscent of Babinet's principle, which says that the diffraction pattern from an opaque object is the same as that from a hole of the same shape, except for the forward beam intensity [12,17]. That the diffraction of the electric field "lost" because of an obstacle is the same as the diffraction of a bright source is the essence of Babinet's principle.

For the probe to not get depleted, I_o must be at least several times bigger than I_{scat} for every path through the atoms. The largest obtainable $I_{sig} \approx I_{scat}/4$, which for our 0.1 numerical aperture imaging lens is 177 times larger than the peak signal from collecting fluorescence. For a given choice of I_o, I_{sig} is proportional to $n_{2D}^2(x,y)$. Since $n_{2D}^2(x,y)$ features are narrower than $n_{2D}(x,y)$ features, the effective resolution of the imaging system is reduced by about a factor of $\sqrt{2}$. From Eq. (6), it is clear that a quantitative measurement of the total atom number requires a quantitative measurement of I_o.

The linearly polarized probe beam is tuned to resonance with the ^{87}Rb D2 transition, $|F=2, m_F\rangle \rightarrow |F'=3, m_F\rangle$ with I_o up to 600 times I_s. To avoid loss to the $|F=1, m_F\rangle$ state via off-resonant scattering from $|F'=2, m_F\rangle$ we repump on the $|F=1, m_F\rangle \rightarrow |F'=2, m_F'\rangle$ transition using a 10% sideband. The atoms therefore spend little time in the $|F=1, m_F\rangle$ state. Also, any light scattered out of the repumping part of the beam has the same effect on the transmitted field as light scattered on the primary transition.

Fig. 2a shows the spatial integral of the detected intensity distribution, S, for an in situ BEC image such as the one shown in Fig. 1a. In the limit of small probe power, the signal intensity increases with power as the probe beam intensity exceeds saturation everywhere and more atoms scatter photons. In the opposite limit, Eq. (6) is valid and the signal intensity decreases with probe power. In between, there is a maximum. Fig. 2b shows the measured root-mean-square (RMS) widths. In the large intensity